

# Probing the Functional Conformation of Neuropeptide Y through the Design and Study of Cyclic Analogues

Marlène Bouvier and John W. Taylor\*

Laboratory of Bioorganic Chemistry and Biochemistry, The Rockefeller University, 1230 York Avenue, New York, New York 10021. Received August 9, 1991

The functional importance of the PP-fold conformation in neuropeptide Y (NPY) was investigated. NPY and  $N^{\alpha}$ -Ac-NPY(10-36), and corresponding cyclic analogues  $cyclo^{18,22}$ -[Lys<sup>18</sup>,Asp<sup>22</sup>]-NPY and  $N^{\alpha}$ -Ac- $cyclo^{18,22}$ -[Lys<sup>18</sup>,Asp<sup>22</sup>]-NPY(10-36), were synthesized. Strategies for synthesis of the cyclic analogues included the use of the Kaiser oxime resin and a segment condensation approach. Circular dichroism studies in phosphate buffer, pH 5.0, indicated self-association of all four peptides at low micromolar concentrations. Monomeric  $N^{\alpha}$ -Ac-NPY(10-36) showed only 13%  $\alpha$ -helix, compared to 32%  $\alpha$ -helix for monomeric NPY, demonstrating a helix-stabilizing effect of residues 1-9 that is consistent with the PP fold. The [Lys<sup>18</sup>,Lys<sup>22</sup>] lactam bridge stabilized the helical conformation in  $N^{\alpha}$ -Ac-NPY(10-36) (51%  $\alpha$ -helix), but was helix destabilizing in NPY (21%  $\alpha$ -helix). In rat brain receptor binding assays, the cyclic and linear  $N^{\alpha}$ -Ac-NPY(10-36) analogues were equipotent ( $IC_{50} = 13$  nM for <sup>125</sup>I-BH-NPY displacement), although the cyclic analogue was twice as potent in rat vas deferens assays. NPY was more potent than its cyclic analogue in the brain receptor binding assays ( $IC_{50} = 0.07$  and 0.25 nM, respectively), but these peptides were equipotent in the vas deferens assays. These results support a functional role for the PP fold in NPY and correlate with the solution conformations of the monomeric peptides.

## Introduction

Determining the functional conformation of linear, biologically active peptides is often a difficult task because of their flexible, multiconformational character in solution and the current inaccessibility of their receptor binding sites using established methods for structural characterization.<sup>1</sup> Nevertheless, identifying these active conformations is a necessary prerequisite to the rational design of potent analogues having improved physicochemical and pharmacological properties, such as increased potency, longer-lasting activity, new receptor specificity, or altered agonist-antagonist character.

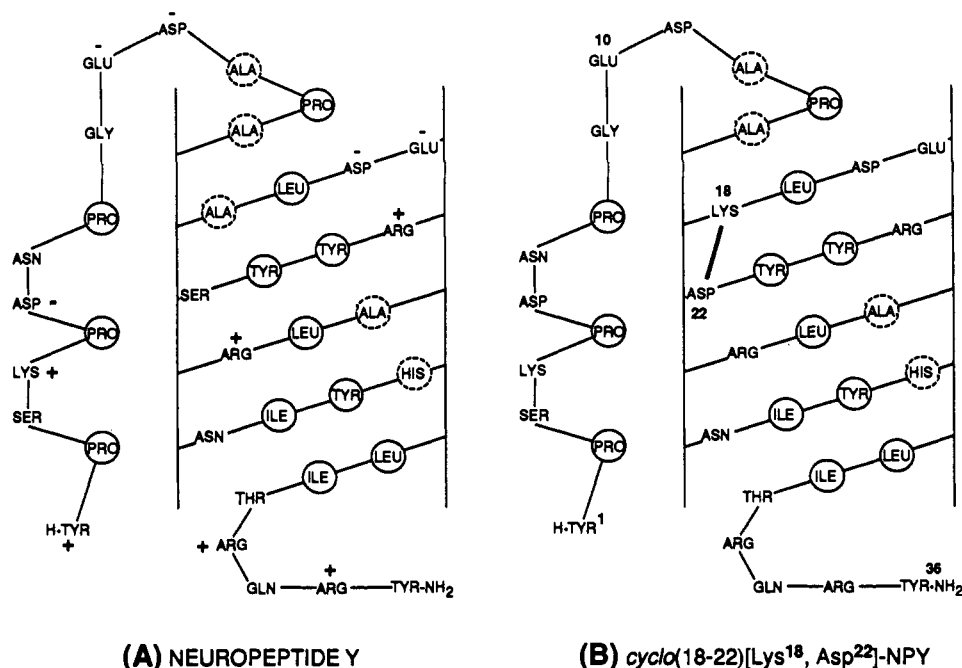
Neuropeptide Y (NPY) is a linear 36-amino acid peptide amide which is structurally analogous to pancreatic polypeptide (PP) and the intestinal hormone peptide YY (PYY).<sup>2</sup> Understanding the molecular basis for the pharmacological activity of NPY is of considerable importance, given its wide distribution in the peripheral and central nervous system.<sup>2,3</sup> Centrally, it influences feeding behavior,<sup>4,5</sup> being the most potent stimulator known, and modulates pituitary hormone secretion.<sup>6</sup> In the periphery, it acts as a potent vasoconstrictor<sup>3,7,8</sup> and inhibitor of neurotransmission.<sup>9</sup>

A distinct tertiary structure, referred to as the PP fold, has been proposed for the PP family, based on the high-resolution X-ray analysis of crystalline avian PP (aPP). The PP fold is a compact, globular structure comprising a left-handed polyproline II-like helix (residues 1-8) that is closely packed through hydrophobic interactions against an amphiphilic  $\alpha$ -helix (residues 13-32).<sup>10,11</sup> In the crystal structure of avian PP, these two antiparallel helices are linked by a  $\beta$ -turn (residues 9-12). The C-terminal region (residues 33-36) adopts no regular structure and extends away from the molecule. Because sequence homology between NPY and aPP conserves the residues that are most important to maintain the integrity of the PP fold, a computer-generated three-dimensional model<sup>12</sup> predicts that NPY also maintains a compact, folded conformation characterized by intramolecular hydrophobic interactions (Figure 1A). This theoretical model is supported by circular dichroism studies, which show that NPY has a relatively high  $\alpha$ -helix content in neutral aqueous solu-

tion,<sup>13</sup> even in the monomeric form,<sup>14</sup> in accordance with a weakly stable, tertiary fold. Recent two-dimensional

\* To whom correspondence should be addressed at the Department of Chemistry, Rutgers University, P.O. Box 939, Piscataway, NJ 08855-0939.

- (1) Taylor, J. W.; Ósapay, G. Determining the Functional Conformations of Biologically Active Peptides. *Acc. Chem. Res.* 1990, 23, 338-344.
- (2) Tatemoto, K. Neuropeptide Y: Complete Amino Acid Sequence of the Brain Peptide. *Proc. Natl. Acad. Sci. U.S.A.* 1982, 79, 5485-5489.
- (3) Lundberg, J. M.; Tatemoto, K. Pancreatic Polypeptide Family (APP, BPP, NPY and PYY) in Relation to Sympathetic Vasoconstriction Resistant to  $\alpha$ -Adrenoceptor Blockade. *Acta Physiol. Scand.* 1982, 116, 393-402.
- (4) Stanley, B. G.; Leibowitz, S. F. Neuropeptide Y Injected in the Paraventricular Hypothalamus: A Powerful Stimulant of Feeding Behavior. *Proc. Natl. Acad. Sci. U.S.A.* 1985, 82, 3940-3943.
- (5) Morley, J. E.; Levine, A. S.; Gosnell, B. A.; Kneip, J.; Grace, M. Effect of Neuropeptide Y on Ingestive Behaviors in the Rat. *Am. J. Physiol.* 1987, 252, R599-R609.
- (6) McDonald, J. K.; Lumpkin, M. D.; Samson, W. K.; McCann, S. M. Neuropeptide Y Affects Secretion of Luteinizing Hormone and Growth Hormone in Ovariectomized Rats. *Proc. Natl. Acad. Sci. U.S.A.* 1985, 82, 561-564.
- (7) Ekblad, E.; Edvinsson, L.; Wahlestedt, C.; Uddman, R.; Hakanson, R.; Sundler, F. Neuropeptide Y Co-exists and Co-operates With Noradrenaline in Perivascular Nerve Fibers. *Regul. Peptides* 1984, 8, 225-235.
- (8) Wahlestedt, C.; Edvinsson, L.; Ekblad, E.; Hakanson, R. Neuropeptide Y Potentiates Noradrenaline-Evoked Vasoconstriction: Mode of Action. *J. Pharmacol. Exp. Ther.* 1985, 234, 735-741.
- (9) Lundberg, J. M.; Stårne, L. Neuropeptide Y (NPY) Depresses the Secretion of <sup>3</sup>H-Noradrenaline and the Contractile Response Evoked by Field Stimulation, in Rat Vas Deferens. *Acta Physiol. Scand.* 1984, 120, 477-479.
- (10) Glover, I.; Haneef, I.; Pitts, J.; Wood, S.; Moss, D.; Tickle, I.; Blundell, T. Conformational Flexibility in a Small Globular Hormone: X-Ray Analysis of Avian Pancreatic Polypeptide at 0.98 Å Resolution. *Biopolymers* 1983, 22, 293-304.
- (11) Glover, I. D.; Barlow, D. J.; Pitts, J. E.; Wood, S. P.; Tickle, I. J.; Blundell, T. L.; Tatemoto, K.; Kimmel, J. R.; Wollmer, A.; Strassberger, W.; Zhang, Y.-S. Conformational Studies on the Pancreatic Polypeptide Hormone Family. *Eur. J. Biochem.* 1985, 142, 379-385.
- (12) Allen, J.; Novotny, J.; Martin, J.; Heinrich, G. Molecular Structure of Mammalian Neuropeptide Y: Analysis by Molecular Cloning and Computer-aided Comparison with Crystal Structure of Avian Homologue. *Proc. Natl. Acad. Sci. U.S.A.* 1987, 84, 2532-2536.
- (13) Krstenansky, J. L.; Buck, S. H. The Synthesis, Physical Characterization and Receptor Binding Affinity of Neuropeptide Y. *Neuropeptides* 1987, 10, 77-85.



(A) NEUROPEPTIDE Y

(B) *cyclo*(18-22)[Lys<sup>18</sup>, Asp<sup>22</sup>]-NPY

**Figure 1.** Structural representation, in the PP fold conformation of (A) NPY and (B) *cyclo*<sup>18,22</sup>-[Lys<sup>18</sup>, Asp<sup>22</sup>]-NPY. Residues 13–32 are represented on a helical net diagram, illustrating the amphiphilic nature of the  $\alpha$ -helix. Positively and negatively charged residues are marked and hydrophobic residues are circled; important residue positions are indicated, and the lactam bridge is represented by a heavy solid line.

NMR studies of NPY in aqueous solution (pH 3.1) also confirm the amphiphilic  $\alpha$ -helical character of the C-terminal region,<sup>15</sup> but indicate that the N-terminal segment adopts no regular structure. However, the state of aggregation of NPY under the conditions of this study was not determined.

Structure-activity relationship studies of NPY indicate that a folded conformation in which the N- and C-terminal residues are in close spatial proximity is important for receptor recognition and activation.<sup>16</sup> For example, although the C-terminal residues appear to be most critical for activity, deletions of N-terminal residues also result in loss of potency in all assays.<sup>17,18</sup> Furthermore, the potency of analogues comprised of the most essential C-terminal residues can be enhanced by connecting them to one or more residues from the N-terminal end of the polypeptide helix via a flexible linking structure.<sup>19,20</sup> Our initial in-

vestigations of NPY have focused on determining the biological importance of the proposed amphiphilic  $\alpha$ -helical structure in residues 13–32.<sup>14</sup> The physicochemical properties of NPY,<sup>13,14</sup> including self-association in aqueous solution, monolayer formation at the air-water interface, and binding to phospholipid vesicles, are all consistent with the presence of an amphiphilic  $\alpha$ -helical surface-binding structure. However, application of a minimal homology modeling approach to designing NPY analogues failed to provide a clear demonstration of the biological importance of this structure: although model peptides having physicochemical properties similar to those of NPY were successfully designed, these analogues were much less potent than the native peptide in receptor binding and rat vas deferens (RVD) assays.<sup>14</sup> Furthermore, even analogues having a low number of conservative substitutions limited to residue positions on either the hydrophilic or hydrophobic face of the helix have greatly reduced potencies.<sup>14,21</sup> Together, these results indicate that, in NPY, a requirement for specific amino acids for expression of biological activity may be superimposed upon the requirement for an amphiphilic  $\alpha$ -helical structure in residues 13–32.

In order to determine the biological importance of the proposed PP fold in NPY, while maintaining the requirement for specific amino acids, we propose to introduce multiple conformational constraints that are designed to be compatible with, and even favor, that particular structural organization.<sup>1</sup> For example, by covalently linking the side chains of pairs of residues that are spatially adjacent to one another in the PP fold, and comparing the

- (14) Minakata, H.; Taylor, J. W.; Walker, M. W.; Miller, R. J.; Kaiser, E. T. Characterization of Amphiphilic Secondary Structures in Neuropeptide Y through the Design, Synthesis, and Study of Model Peptides. *J. Biol. Chem.* 1989, **264**, 7907–7913.
- (15) Saudek, V.; Pelton, J. T. Sequence-specific <sup>1</sup>H-NMR Assignment and Secondary Structure of Neuropeptide Y in Aqueous Solution. *Biochemistry* 1990, **29**, 4509–4515.
- (16) Fuhlendorff, J.; Johansen, N. L.; Melberg, S. G.; Thøgersen, H.; Schwartz, T. W. The Antiparallel Pancreatic Polypeptide Fold in the Binding of Neuropeptide Y to Y<sub>1</sub> and Y<sub>2</sub> receptors. *J. Biol. Chem.* 1990, **265**, 11706–11712.
- (17) Danho, W.; Triscari, J.; Vincent, G.; Nakajima, T.; Taylor, J.; Kaiser, E. T. Synthesis and Biological Evaluation of pNPY Fragments. *Int. J. Pept. Protein Res.* 1988, **32**, 496–505.
- (18) Rioux, F.; Bachelard, H.; Martel, J.-C.; St-Pierre, S. The Vasoconstrictor Effect of Neuropeptide Y and Related Peptides in the Guinea Pig Isolated Heart. *Peptides* 1986, **7**, 27–31.
- (19) Beck-Sickinger, A. G.; Jung, G.; Gaida, W.; Köppen, H.; Schnorrenberg, G.; Lang, R. Structure/Activity Relationships of C-Terminal Neuropeptide Y Peptide Segments and Analogues Composed of Sequence 1–4 Linked to 25–36. *Eur. J. Biochem.* 1990, **194**, 449–456.

- (20) Krstenansky, J. L.; Owen, T. J.; Buck, S. H.; Hagaman, K. A.; McLean, L. R. Centrally Truncated and Stabilized Porcine Neuropeptide Y Analogs: Design, Synthesis, and Mouse Brain Receptor Binding. *Proc. Natl. Acad. Sci. U.S.A.* 1989, **86**, 4377–4381.
- (21) Martel, J.-C.; Fournier, A.; St-Pierre, S.; Dumont, Y.; Forest, M.; Quirion, R. Comparative Structural Requirements of Brain Neuropeptide Y Binding Site and Vas Deferens Neuropeptide Y Receptors. *Mol. Pharmacol.* 1990, **38**, 494–502.

pharmacological properties of the resulting multicyclic peptides with those of the corresponding acyclic analogues, we expect to obtain more direct and conclusive information on the biological role of the PP fold in NPY.

In a first step toward this goal, we have developed a segment-condensation strategy<sup>22,23</sup> for the synthesis of multicyclic peptides that is based on solid-phase synthesis using the Kaiser oxime resin.<sup>24,25</sup> This synthetic approach has now been used to prepare two analogues of NPY that incorporate a lactam bridge formed between the side chains of lysine and aspartic acid residues substituted into the proposed  $\alpha$ -helical structure in positions 18 and 22, respectively. Lactam bridges linking Lys<sup>n</sup> to Asp<sup>n+4</sup> or Asp<sup>n</sup> to Lys<sup>n+4</sup> have previously been shown to stabilize the  $\alpha$ -helical conformation in analogues of growth hormone (GRF) releasing factor<sup>26,27</sup> and in model amphiphilic  $\alpha$ -helical peptides.<sup>28</sup> In the present study, the syntheses of *N*<sup>α</sup>-Ac-cyclo<sup>18,22</sup>-[Lys<sup>18</sup>,Asp<sup>22</sup>]-NPY(10-36) and cyclo<sup>18,22</sup>-[Lys<sup>18</sup>,Asp<sup>22</sup>]-NPY (Figure 1B) are described and the physicochemical and pharmacological properties of these cyclic analogues are compared with those of the corresponding unsubstituted, linear peptides.

## Results

**Peptide Design.** Analogues of NPY and *N*<sup>α</sup>-Ac-NPY-(10-36) having a lactam bridge formed by the side-chain to side-chain cyclization of [Lys<sup>18</sup>] and [Asp<sup>22</sup>] (Figure 1B) were synthesized and their physicochemical and pharmacological properties were compared with those of the corresponding linear peptides. The lactam bridge structure was chosen on the basis of previous results for its expected  $\alpha$ -helix stabilizing properties.<sup>26-28</sup> Positions 18 and 22 were selected for substitutions because these residues (Ala<sup>18</sup> and Ser<sup>22</sup>) are not conserved in the sequence of PYY (Ser<sup>18</sup> and Ala<sup>22</sup>), which nevertheless binds to NPY receptors with high affinity.<sup>29</sup> This suggests a minor functional role for these residues in expressing the biological activity of NPY. *N*<sup>α</sup>-Ac-NPY(10-36) was designed to study the  $\alpha$ -helix stabilizing effect of the N-terminal polyproline II-like helix

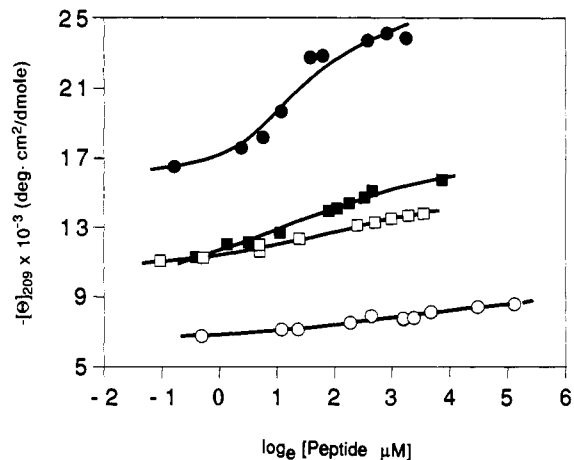


**Figure 2.** Concentration dependence of the molar ellipticity (10 mM phosphate buffer, pH 5.0) at 209 nm for *N*<sup>α</sup>-Ac-NPY(10-36) (○); *N*<sup>α</sup>-Ac-cyclo<sup>18,22</sup>-[Lys<sup>18</sup>,Asp<sup>22</sup>]-NPY(10-36) (●); NPY (□); cyclo<sup>18,22</sup>-[Lys<sup>18</sup>,Asp<sup>22</sup>]-NPY (■). The solid lines were determined by curve-fitting analyses of the data points according to the appropriate cooperative monomer-oligomer equilibrium described by eq 1 (see text).

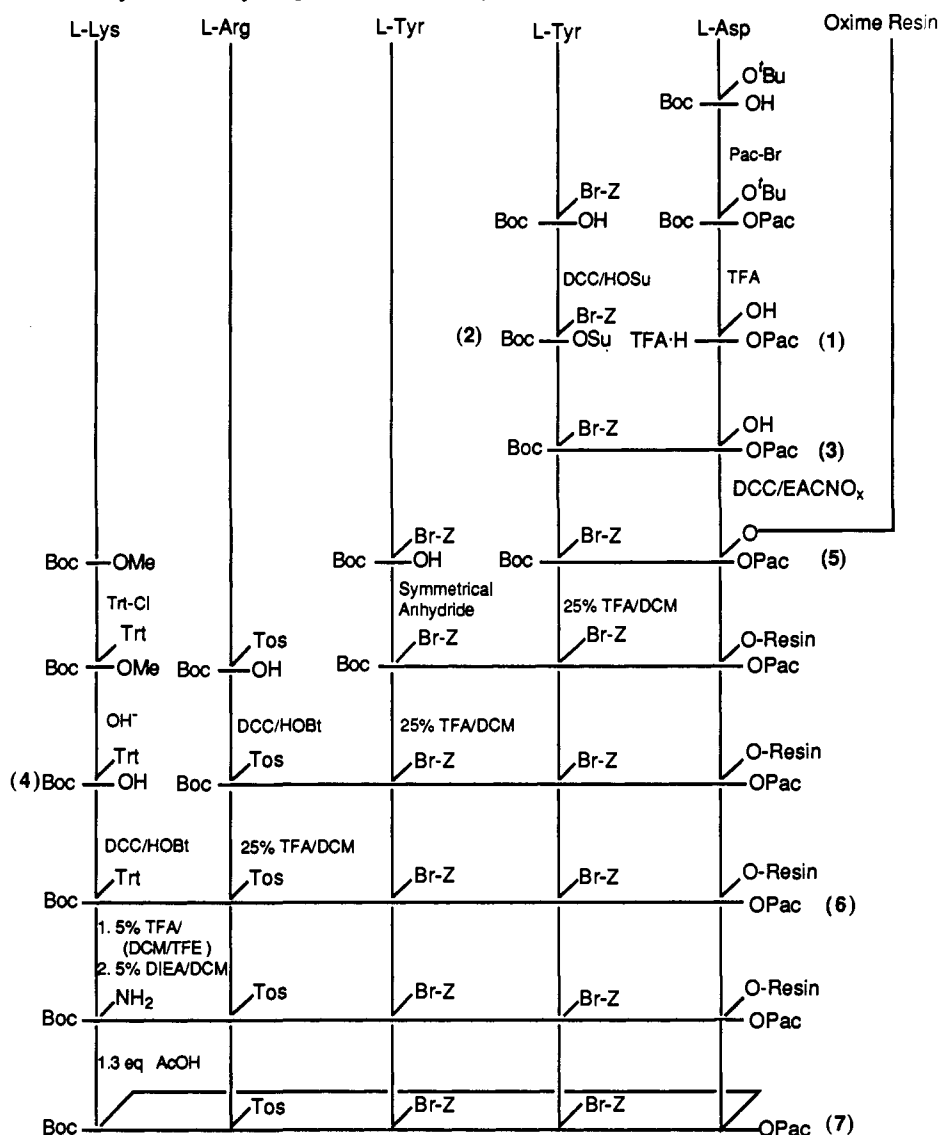
on the amphiphilic  $\alpha$ -helical domain as proposed in the PP fold. The introduction of a conformational constraint in this analogue serves two main purposes: first, to confirm the stabilizing effect of a single lactam bridge of the type Lys<sup>n</sup>, Asp<sup>n+4</sup> on the  $\alpha$ -helical conformation, and second, to study the biological importance of this secondary structure in NPY. Both truncated analogues were *N*<sup>α</sup>-acetylated to prevent the introduction of a positive charge at the N-terminal amino group.

**Peptide Synthesis.** The strategy used for the synthesis of the protected cyclic peptide 7 was based on the particular features that characterize the Kaiser oxime resin.<sup>24,25</sup> This support is generally used for the solid-phase synthesis of linear protected peptides to be coupled in solution or on solid supports.<sup>30,31</sup> However, the anchoring oxime ester bond can also be used as a polymeric active ester for the cyclization of protected peptides that are concomitantly released into solution. This strategy has been applied successfully to the syntheses of various head-to-tail and side-chain to side-chain cyclic peptides in high yield and purity.<sup>22,32</sup>

Protected cyclic peptide 7 was synthesized on oxime resin, as described in Scheme I. The key steps in this synthesis are the selective deprotection of *N*<sup>α</sup>-Trt, which was followed by absorbance measurements and judged nearly quantitative after 3 h, and the subsequent cyclization/cleavage reaction. This latter step resulted in a mixture of the desired peptide 7 and the corresponding covalent dimer in a molar ratio of 4:1, respectively, with a 43% overall yield. Purified peptide 7 was then C<sup>α</sup>-deprotected and condensed with the protected sequence NH<sub>2</sub>-(NPY(23-36))-*p*-MBHA resin in 60% yield, as described in Scheme II. Repetitive solid-phase coupling cycles on the resulting peptidyl resin 9, followed by HF

- (22) Ósabay, G.; Taylor, J. W. Multicyclic Polypeptide Model Compounds. 1. Synthesis of a Tricyclic Amphiphilic  $\alpha$ -Helical Peptide Using an Oxime Resin, Segment-Condensation Approach. *J. Am. Chem. Soc.* 1990, 112, 6046-6051.
- (23) Ósabay, G.; Bouvier, M.; Taylor, J. W. Peptide Cyclization on Oxime Resin (PCOR). In *Techniques in Protein Chemistry II*; Villafranca, J. J., Ed.; Academic Press: San Diego, 1991; pp 221-231.
- (24) DeGrado, W. F.; Kaiser, E. T. Polymer-Bound Oxime Esters as Supports for Solid-Phase Peptide Synthesis. Preparation of Protected Peptide Fragments. *J. Org. Chem.* 1980, 45, 1295-1300.
- (25) DeGrado, W. F.; Kaiser, E. T. Solid-Phase Synthesis of Protected Peptides on a Polymer-Bound Oxime: Preparation of Segments Comprising the Sequence of a Cytotoxic 26-Peptide Analogue. *J. Org. Chem.* 1982, 47, 3258-3261.
- (26) Felix, A. M.; Heimer, E. P.; Wang, C.-T.; Lambros, T. J.; Fournier, A.; Mowles, T. F.; Maines, S.; Campbell, R. M.; Wegrzynski, B. B.; Toome, V.; Fry, D.; Madison, V. S. Synthesis, Biological Activity and Conformational Analysis of Cyclic GRF Analogs. *Int. J. Pept. Protein Res.* 1988, 32, 441-454.
- (27) Madison, V. S.; Fry, D. C.; Greeley, D. N.; Toome, V.; Wegrzynski, B. B.; Heimer, E. P.; Felix, A. M. Conformational Analysis of Bioactive Analogs of Growth Hormone-Releasing Factor (GRF). In *Peptides: Chemistry, Structure and Biology*, Proc. 11th Amer. Peptide Symp.; Rivier, J. E., Marshall, G. R., Eds.; Escom: Leiden, 1990; pp 575-577.
- (28) Ósabay, G.; Gulyás, J.; Profit, A.; Gulyás, E.; Taylor, J. W. In *Proc. 12th Am. Peptide Symp.*, in press.
- (29) Walker, M. W.; Miller, R. J. <sup>125</sup>I-Neuropeptide Y and <sup>125</sup>I-Peptide YY Bind to Multiple Receptor Sites in Rat Brain. *Mol. Pharmacol.* 1988, 34, 779-792.

- (30) Sasaki, T.; Findeis, M. A.; Kaiser, E. T. Evaluation of The Oxime Resin Based Segment Synthesis-Condensation Approach Using RNase T<sub>1</sub> as a Model Synthetic Target. *J. Org. Chem.* 1991, 56, 3159-3168.
- (31) Kaiser, E. T.; Mihara, H.; Laforet, G. A.; Kelly, J. W.; Walters, L.; Findeis, M. A.; Sasaki, T. Peptide and Protein Synthesis by Segment Synthesis-Condensation. *Science* 1989, 243, 187-192.
- (32) Ósabay, G.; Profit, A.; Taylor, J. W. Synthesis of Tyrocidine A: Use of Oxime Resin for Peptide Chain Assembly and Cyclization. *Tetrahedron Lett.* 1990, 31, 6121-6124.

Scheme I. Synthetic Route to *cyclo*<sup>1,5</sup>-Boc-Lys-Arg(Tos)-Tyr(Br-Z)-Tyr(Br-Z)-Asp-OPac (7)

cleavage and reverse-phase HPLC purification of the crude peptides, gave the desired lactam-bridged peptides 10 and 11. The corresponding linear peptides 12 and 13 were synthesized according to the standard protocol for stepwise solid-phase synthesis and purification by reverse-phase HPLC. All peptides had the expected amino acid composition and correct molecular mass.

**Circular Dichroism Studies.** All four peptides show CD spectra that are indicative of different mixtures of helix and disordered conformations in 10 mM sodium phosphate (pH 5.0). In the concentration range from 0.35 to 171  $\mu$ M, the spectra show a concentration dependency and are also indicative of self-association with concomitant  $\alpha$ -helix stabilization, a general characteristic of amphiphilic  $\alpha$ -helical peptides.<sup>33</sup> *N* <sup>$\alpha$</sup> -Ac-NPY(10-36) appears to have the lowest helical content in this concentration range, based on the magnitude of the negative mean residue ellipticities at 209 and 222 nm.<sup>34</sup> However, the corresponding lactam-bridged analogue, *N* <sup>$\alpha$</sup> -Ac-*cyclo*<sup>18,22</sup>-

[Lys<sup>18</sup>,Asp<sup>22</sup>]-NPY(10-36), shows the highest helical content and the most pronounced concentration dependency (Figure 2). The helical contents and concentration dependencies observed for NPY and *cyclo*<sup>18,22</sup>-[Lys<sup>18</sup>,Asp<sup>22</sup>]-NPY are, in contrast, very comparable and intermediate in magnitude between those of the truncated analogues.

Using the methods described by Kaumaya et al.,<sup>35</sup> the mean residue ellipticity data at 209 nm were fit by tri-variant nonlinear regression analysis (Kaleidagraph, Synergy Software) to a general equation describing a cooperative monomer-oligomer equilibrium:

$$\ln [P] = \ln (\theta_{\text{olig}} - \theta_{\text{mon}}) + [1/(n-1)] \ln (K_D/n) + [1/(n-1)] \ln (\theta_{\text{exp}} - \theta_{\text{mon}}) - [n/(n-1)] \ln (\theta_{\text{olig}} - \theta_{\text{exp}}) \quad (1)$$

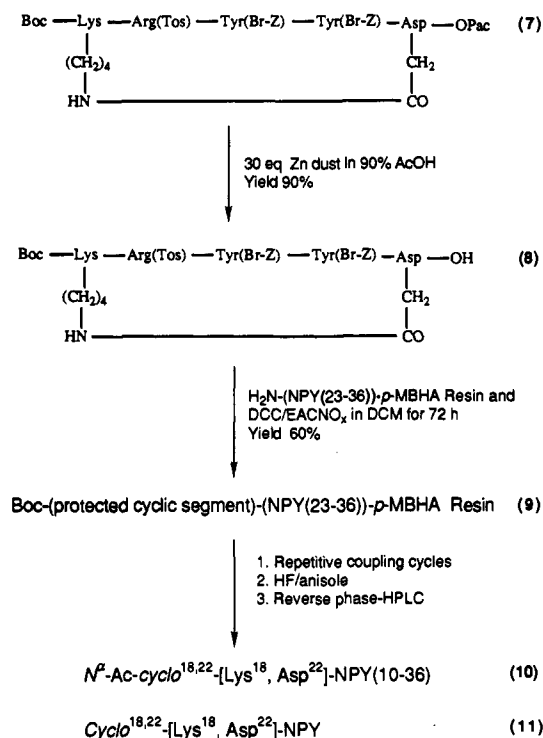
where  $\theta_{\text{exp}}$  is the experimental mean residue ellipticity at 209 nm,  $\theta_{\text{mon}}$  and  $\theta_{\text{olig}}$  are the theoretical mean residue ellipticities of the monomer and oligomer, respectively,  $K_D$  is the apparent dissociation constant for the monomer-

(33) Taylor, J. W.; Kaiser, E. T. Structure-Function Analysis of Proteins Through the Design, Synthesis, and Study of Peptide Models. *Methods Enzymol.* 1987, 154, 473-498.

(34) Greenfield, N.; Fasman, G. D. Computed Circular Dichroism Spectra for the Evaluation of Protein Conformation. *Biochemistry* 1969, 8, 4108-4116.

(35) Kaumaya, P. T. P.; Berndt, K. D.; Heidorn, D. B.; Trehwella, J.; Kedzy, F. J.; Goldberg, E. Synthesis and Biophysical Characterization of Engineered Topographic Immunogenic Determinants with  $\alpha\alpha$  Topology. *Biochemistry* 1990, 29, 13-23.

**Scheme II.** Combined Stepwise and Segment Condensation Solid-Phase Synthesis of  $N^{\alpha}$ -Ac-cyclo<sup>18,22</sup>-[Lys<sup>18</sup>, Asp<sup>22</sup>]-NPY(10-36) (10) and cyclo<sup>18,22</sup>-[Lys<sup>18</sup>, Asp<sup>22</sup>]-NPY (11)



oligomer complex, [P] the total concentration of peptide, and  $n$  the degree of self-association. A value of  $n$  was initially obtained from the slope of a plot of  $\ln$  [oligomer] versus  $\ln$  [monomer] as described by the following equation:

$$\ln [\text{oligomer}] = n \ln [\text{monomer}] - \ln (K_D) + \ln (n) \quad (2)$$

where

$$[\text{oligomer}] = [P] (\theta_{\text{exp}} - \theta_{\text{mon}}) / (\theta_{\text{olig}} - \theta_{\text{mon}})$$

$$[\text{monomer}] = [P] (\theta_{\text{olig}} - \theta_{\text{exp}}) / (\theta_{\text{olig}} - \theta_{\text{mon}})$$

and values for  $\theta_{\text{mon}}$  and  $\theta_{\text{olig}}$  were estimated by extrapolating the experimental points in Figure 2. This value of  $n$  was then rounded to the nearest whole number and used in eq 1 to obtain values for  $\theta_{\text{mon}}$ ,  $\theta_{\text{olig}}$ , and  $K_D$  that best fit the experimental data for each peptide.

Analysis of the data for  $N^{\alpha}$ -Ac-NPY(10-36) according to eq 2 gives  $n = 1.98$  (correlation coefficient,  $r^2 = 0.984$ ), indicating that the behavior of the linear truncated peptide is best described by a monomer-dimer equilibrium. Optimal fits of this data to eq 1 with  $n = 2$  gave  $\theta_{\text{mon}} = -6660 \text{ deg}\cdot\text{cm}^2/\text{dmol}$ ,  $\theta_{\text{olig}} = -9410 \text{ deg}\cdot\text{cm}^2/\text{dmol}$ , and  $K_D = 32 \text{ }\mu\text{M}$ , which corresponds to a free energy of dimerization of  $-6.13 \text{ kcal/mol}$  dimer (Table I). The corresponding lactam-bridged peptide,  $N^{\alpha}$ -Ac-cyclo<sup>18,22</sup>-[Lys<sup>18</sup>, Asp<sup>22</sup>]-NPY(10-36) is described by a monomer-tetramer equilibrium based on eq 2 with  $n = 3.76$  ( $r^2 = 0.893$ ). Values of  $\theta_{\text{mon}} = -16470 \text{ deg}\cdot\text{cm}^2/\text{dmol}$ ,  $\theta_{\text{olig}} = -25990 \text{ deg}\cdot\text{cm}^2/\text{dmol}$ , and  $K_D = 4.4 \times 10^{-17} \text{ M}^3$ , i.e.,  $44 (\mu\text{M})^3$  corresponding to a free energy of tetramerization of  $-22.3 \text{ kcal/mol}$  tetramer, were obtained from analysis of the data according to eq 1. The curve-fitting analysis also confirmed the closely related concentration dependencies and conformations of NPY and cyclo<sup>18,22</sup>-[Lys<sup>18</sup>, Asp<sup>22</sup>]-NPY (Table I). Values of  $n = 1.96$  ( $r^2 = 0.994$ ) and  $n = 1.94$  ( $r^2 = 0.994$ ), respectively, were obtained for these peptides on the basis of eq 2. Very similar values for  $\theta_{\text{mon}}$ ,  $\theta_{\text{olig}}$ , and  $K_D$  were generated for these

**Table I.** Parameters Characterizing Cooperative Monomer-Oligomer Equilibria for Peptides

peptides	$-\theta_{\text{mon}}$ (deg·cm <sup>2</sup> / dmol)	$-\theta_{\text{olig}}$ (deg·cm <sup>2</sup> / dmol)	$K_D$	$n$	$\Delta G_{\text{mon-olig}}$ (kcal/mol)
$N^{\alpha}$ -Ac-NPY(10-36)	6660	9410	32 $\mu\text{M}$	2	-6.1
$N^{\alpha}$ -Ac-cyclo <sup>18,22</sup> - [Lys <sup>18</sup> , Asp <sup>22</sup> ]- NPY(10-36)	16470	25990	44 ( $\mu\text{M}$ ) <sup>3</sup>	4	-22.3
NPY	10670	14740	11 $\mu\text{M}$	2	-6.8
cyclo <sup>18,22</sup> - [Lys <sup>18</sup> , Asp <sup>22</sup> ]- NPY	9900	17340	5.4 $\mu\text{M}$	2	-7.2

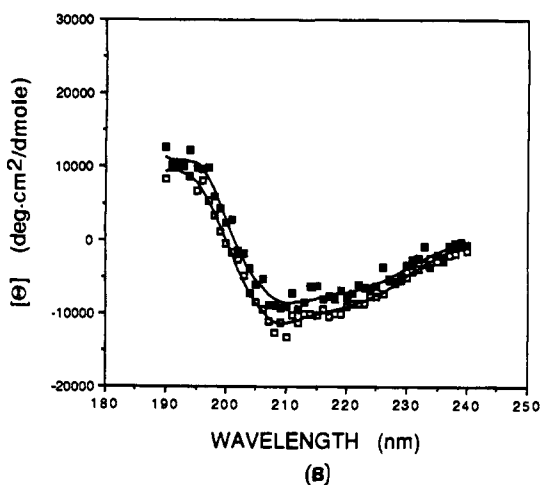
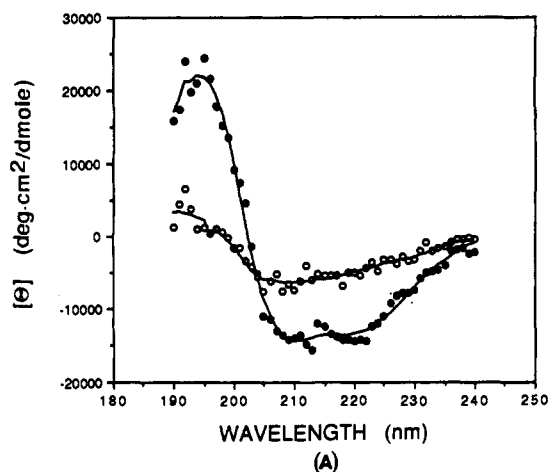


**Figure 3.** Circular dichroism spectra (10 mM phosphate buffer, pH 5.0) of the monomeric forms of (A)  $N^{\alpha}$ -Ac-NPY(10-36) (1.0  $\mu\text{M}$ ) (O) and  $N^{\alpha}$ -Ac-cyclo<sup>18,22</sup>-[Lys<sup>18</sup>, Asp<sup>22</sup>]-NPY(10-36) (0.83  $\mu\text{M}$ ) (●); (B) NPY (0.70  $\mu\text{M}$ ) (□) and cyclo<sup>18,22</sup>-[Lys<sup>18</sup>, Asp<sup>22</sup>]-NPY (0.65  $\mu\text{M}$ ) (■). Theoretical lines through the data points were generated from a computational fit by the method of Provencher and Glöckner.<sup>36</sup>

two analogues as best fits to eq 1 (Table I). However, whereas analysis of the data using eq 2 to generate the degree of self-association of the peptides distinguished very well between different possible values of  $n$  in the case of the truncated analogues, it was somewhat less discriminatory for the full-length analogues and values of  $n = 2$  or  $n = 3$  fit almost equally well. However, the use of  $n = 2$  or  $n = 3$  in eq 1 generated very similar values of  $\theta_{\text{mon}}$  for the full-length analogues, the parameter that characterizes the biologically active form of these peptides.

Circular dichroism spectra corresponding to the monomeric and pharmacologically active form of the peptides were recorded in the range from 240 to 190 nm in order to determine secondary structure contents (Figure 3).

**Table II.** Secondary Structure Compositions of Peptides

peptide	concn ( $\mu$ M)	% $\alpha$ -helix <sup>a</sup>	% $\beta$ -sheet <sup>a</sup>	% $\beta$ -turn <sup>a</sup>	% remainder <sup>a</sup>	% $\alpha$ -helix <sup>b</sup>
<i>N</i> <sup>α</sup> -Ac-NPY(10-36)						
monomer	1.0	13	43	23	21	19
dimer	94	24	28	20	27	26
<i>N</i> <sup>α</sup> -Ac-cyclo <sup>18,22</sup> -[Lys <sup>18</sup> ,Asp <sup>22</sup> ]-NPY(10-36)						
monomer	0.83	51	22	13	15	43
tetramer	33	96	0	0	4	74
NPY						
monomer	0.70	32	31	18	20	30
dimer <sup>c</sup>	42	36	26	16	21	33
cyclo <sup>18,22</sup> -[Lys <sup>18</sup> ,Asp <sup>22</sup> ]-NPY						
monomer	0.65	21	40	19	20	25
dimer <sup>c</sup>	22	36	27	18	20	32

<sup>a</sup>Determined by analysis of the CD spectra in 10 mM phosphate buffer, pH 5.0, using the method of Provencher and Glöckner.<sup>36</sup>  
<sup>b</sup>Calculated from  $[\theta]_{222}$  (deg-cm<sup>2</sup>/dmol) using the formula % helix = 100%  $\times$  ( $[\theta]_{222} - 3000$ )/-39000.<sup>34</sup> <sup>c</sup>Analysis of the data in Figure 2 indicates dimerization at this concentration, but cooperative trimerization cannot be ruled out (see text).

**Table III.** Receptor Binding and Rat Vas Deferens Activities of Peptides

peptides	receptor binding activity:	
	IC <sub>50</sub> (nM) <sup>a</sup>	RVD activity: IC <sub>50</sub> (nM) <sup>b</sup>
<i>N</i> <sup>α</sup> -Ac-NPY(10-36)	13 $\pm$ 3	103 $\pm$ 12
<i>N</i> <sup>α</sup> -Ac-cyclo <sup>18,22</sup> -[Lys <sup>18</sup> ,Asp <sup>22</sup> ]-NPY(10-36)	13 $\pm$ 2	49 $\pm$ 7
NPY	0.070 $\pm$ 0.02	17 $\pm$ 1
cyclo <sup>18,22</sup> -[Lys <sup>18</sup> ,Asp <sup>22</sup> ]-NPY	0.25 $\pm$ 0.06	16 $\pm$ 3

<sup>a</sup>Values represent the mean  $\pm$  SEM of three to seven independent experiments done in triplicate. <sup>b</sup>Values represent the mean  $\pm$  SEM of three to seven independent experiments.

Figure 3A illustrates the marked contrast between the CD spectrum of the lactam-bridged truncated analogue, which is characterized by two distinct minima at 209 and 222 nm indicative of a high  $\alpha$ -helix content, and that of the corresponding acyclic analogue, which indicates very little  $\alpha$ -helical structure. These results clearly demonstrate the inherent potential of a single Lys<sup>n</sup>, Asp<sup>n+4</sup> bridge to stabilize the  $\alpha$ -helical conformation. However, a different result is obtained from a comparison of the CD spectra of cyclo<sup>18,22</sup>-[Lys<sup>18</sup>,Asp<sup>22</sup>]-NPY and NPY (Figure 3B). In this particular case, the CD spectrum of the monomeric cyclic analogue is somewhat less negative at 209 and 222 nm than that of NPY. This suggests that introduction of the Lys<sup>18</sup>,Asp<sup>22</sup> lactam bridge in NPY structure destabilizes the helical conformation.

Secondary structure compositions for each peptide monomer were estimated from computational fits of the CD spectra in Figure 3 by the method of Provencher and Glöckner<sup>36</sup> (Table II). A similar analysis of the CD spectra of each peptide measured at higher concentrations, where the oligomeric form is predominant, was also performed. The results of this type of analysis are best interpreted by relative comparisons, and the values for  $\alpha$ -helix content are expected to be more accurate than those for other conformations since the CD signal for helix is by far the most intense signal in this wavelength range. Furthermore, as was noted previously,<sup>14</sup> possible contributions to the CD spectra of NPY and its cyclic analogue due to the polyproline II-like helical structure proposed for residues 1-8 in the PP fold conformation are not properly accounted for in these computations. To confirm our qualitative interpretations of the CD spectra for the full-length peptides, we have therefore also calculated helix contents from

the mean residue ellipticity at 222 nm, using an approximation based on the spectra of polylysine in random and  $\alpha$ -helical conformations<sup>34</sup> that was applied to our earlier studies of NPY and NPY analogues<sup>14</sup> (Table II). The CD spectrum of NPY residues 1-8 in the polyproline II conformation is expected to be similar in shape to the CD spectrum of collagen rather than polyproline itself, in view of the reduced proline content of the NPY structure,<sup>16,37</sup> with a strong minimum at 197 nm, a crossover point from negative to positive ellipticity at 213 nm, and a weaker maximum around 223 nm. However, the intensity of this spectrum is uncertain, and model peptide studies suggest that it may be significantly lower for the more flexible single-stranded structure in this conformation than for the triple-helical collagen structure.<sup>37</sup> The contribution to the CD signal at 222 nm due to any polyproline II-like structure should, therefore, be small and positive, as is that of the "random" structure of polylysine upon which the percent helix estimation is based.

In the case of the N-terminal-deleted peptides, a 13%  $\alpha$ -helix content is estimated for the monomeric linear analogue by the Provencher and Glöckner method, whereas that for the monomeric cyclic peptide is approximately 4 times higher. For both of these peptides, the oligomeric form has nearly double the  $\alpha$ -helix content of the monomeric form. A value of 32%  $\alpha$ -helix content is estimated for the monomer of NPY by the same method (Table II). This value is similar to those previously reported for monomeric NPY in aqueous saline solutions at higher pH.<sup>13,14</sup> A reduced  $\alpha$ -helix content is obtained for monomeric cyclo<sup>18,22</sup>-[Lys<sup>18</sup>,Asp<sup>22</sup>]-NPY (21%) in comparison to monomeric NPY, although the  $\alpha$ -helix contents calculated for the dimeric forms of these peptides are identical (36%). Qualitatively similar results were obtained for all of the monomeric peptides by estimating percent  $\alpha$ -helix from the mean residue ellipticity at 222 nm in comparison to the spectra of polylysine.<sup>34</sup> This indicates that effects on the estimated percent  $\alpha$ -helix by the Provencher and Glöckner method of possible polyproline II-like structures

(36) Provencher, S. W.; Glöckner, J. Estimation of Globular Secondary Structure from Circular Dichroism. *Biochemistry* 1981, 20, 33-37.

(37) Brown, F. R., III; Di Corato, A.; Lorenzi, G. P.; Blout, E. R. Synthesis and Structural Studies of Two Collagen Analogues: Poly(L-prolyl-L-seryl-glycyl) and Poly(L-prolyl-L-alanyl-glycyl). *J. Mol. Biol.* 1972, 63, 85-99. Attempts at deconvoluting the CD spectra for monomeric NPY and cyclo<sup>18,22</sup>-[Lys<sup>18</sup>,Asp<sup>22</sup>]-NPY using least squares methods and including the collagen spectrum described in ref 16 in the basis sets of spectra gave poor results that appeared to underestimate  $\alpha$ -helix and overestimate  $\beta$ -sheet: this curve fitting did not properly account for the minima at 209 nm in these spectra, whereas those from the Provencher and Glöckner analysis fit well in this region and throughout all of the spectra (Figure 3B).

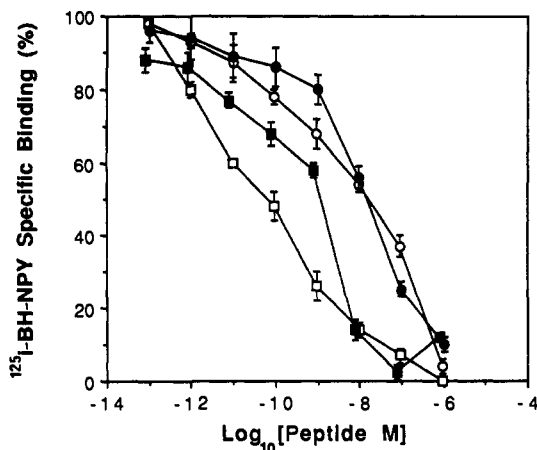


**Figure 4.** Competitive displacement of  $^{125}\text{I}$ -BH-NPY in rat cortical membranes by  $N^{\alpha}$ -Ac-NPY(10-36) (O);  $N^{\alpha}$ -Ac-cyclo $^{18,22}$ -[Lys $^{18}$ ,Asp $^{22}$ ]-NPY(10-36) (●); NPY (□); cyclo $^{18,22}$ -[Lys $^{18}$ ,Asp $^{22}$ ]-NPY (■). Each point represents the mean  $\pm$  SEM of three to seven independent experiments in which each point was determined in triplicate. Results are expressed as percentage of the specific radioligand binding.

in NPY and cyclo $^{18,22}$ -[Lys $^{18}$ ,Asp $^{22}$ ]-NPY are small.

**Sedimentation Equilibrium Experiments.** Sedimentation equilibrium experiments were performed as a direct way of determining the degree of self-association of peptides. However, in nearly all experiments performed, the graph of  $\ln$  absorbance versus (radial distance) $^2$  was characterized by a nonlinear relationship. This result confirms the aggregation behavior observed by CD for these peptides in the micromolar concentration range and suggests that they behave as mixed molecular species under the conditions of the experiments. Similar results have previously been reported for NPY, $^{13}$  and higher peptide concentrations appear to be required to determine the correct value of  $n$  by sedimentation equilibrium analysis. (The use of hemoglobin solution as a standard ensured the reliability of these experiments.)

**Receptor Binding Assays.** The results from competitive ( $^{125}\text{I}$ -BH-NPY) receptor binding experiments in rat cortical membranes are presented in Figure 4, and  $\text{IC}_{50}$  values obtained from analysis of the data are given in Table III. The results indicate that all of the peptides compete for receptor binding in the low nanomolar range. The N-terminal deleted peptides show identical  $\text{IC}_{50}$  values (13 nM), suggesting that the [Lys $^{18}$ ,Asp $^{22}$ ] bridge is compatible with the receptor-bound conformation of  $N^{\alpha}$ -Ac-NPY(10-36). Furthermore, both peptides are significantly less potent than either of the full-length peptides. However, a comparison of the competitive binding properties of the two full-length peptides (Table III) does not support the conclusion derived for the two truncated analogues. Indeed, cyclo $^{18,22}$ -[Lys $^{18}$ ,Asp $^{22}$ ]-NPY shows a slightly weaker ability ( $\text{IC}_{50} = 0.25$  nM) to compete with the radioligand for receptor binding than NPY ( $\text{IC}_{50} = 0.070$  nM), suggesting that, in this case, the lactam bridge does interfere somewhat with receptor recognition.

**Rat Vas Deferens Assays.** Figure 5 shows the log dose-response curves for each peptide on the rat vas deferens. All four peptides are capable of almost completely inhibiting the electrically stimulated contractions of the rat vas deferens and are therefore characterized by comparable intrinsic activities approaching 100%. The N-terminal deleted peptides are both less potent than the full-length peptides. In this assay, however, the cyclic truncated analogue ( $\text{IC}_{50} = 49$  nM) was significantly more potent than the corresponding linear peptide ( $\text{IC}_{50} = 103$

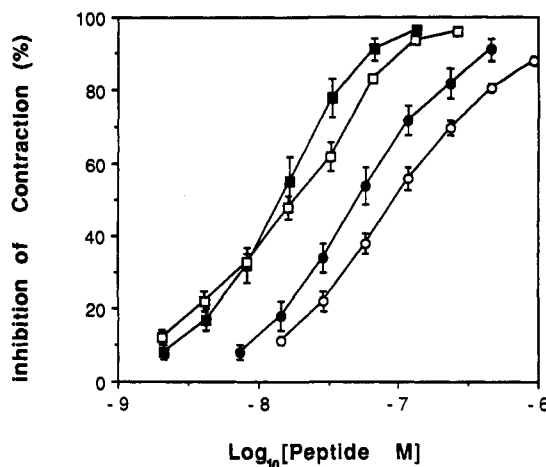


**Figure 5.** Dose-response curves on the rat vas deferens for  $N^{\alpha}$ -Ac-NPY(10-36) (O);  $N^{\alpha}$ -Ac-cyclo $^{18,22}$ -[Lys $^{18}$ ,Asp $^{22}$ ]-NPY(10-36) (●); NPY (□); cyclo $^{18,22}$ -[Lys $^{18}$ ,Asp $^{22}$ ]-NPY (■). Each point represents the mean  $\pm$  SEM of three to seven independent experiments. Results are expressed as percentage of the maximal inhibitory response.

nM) (Table III), so that potency correlates with helix stabilization. In the case of the full-length peptides, equipotency on the rat vas deferens is obtained as indicated by the  $\text{IC}_{50}$  values (Table III). However, the dose-response curves (Figure 5) indicate that the cyclic analogue is slightly more potent than NPY at concentrations above the  $\text{IC}_{50}$ .

## Discussion

The PP fold, $^{10,11}$  comprising an N-terminal polyproline II-like helix (residues 1-8) packed in an antiparallel orientation against the hydrophobic face of an amphiphilic  $\alpha$ -helix (residues 13-32), has been proposed as the active conformation of NPY. $^{14,16,19,38}$  In the context of receptor recognition, this conformation has several attractive features. The PP fold brings N- and C-terminal residues that are known to be important for receptor recognition and specificity into close spatial proximity; it creates a strong electric dipole that would generate complementary long-range electrostatic interactions with a negatively charged receptor binding surface and orient the NPY molecule in the correct fashion for receptor recognition; the amphiphilic character of the two helical components might enhance the affinity of NPY for receptor surfaces in aqueous media.

In order to study the importance of the PP-fold conformation of NPY in aqueous solution, and its functional importance in determining the pharmacological properties of NPY, four peptides were synthesized: NPY,  $N^{\alpha}$ -Ac-NPY(10-36), and two conformationally constrained cyclic analogues, cyclo $^{18,22}$ -[Lys $^{18}$ ,Asp $^{22}$ ]-NPY and  $N^{\alpha}$ -Ac-cyclo $^{18,22}$ -[Lys $^{18}$ ,Asp $^{22}$ ]-NPY(10-36). Cyclic peptides were synthesized using the Kaiser oxime resin combined with a segment-condensation approach. $^{22}$  This approach was chosen over others $^{26}$  because it can eventually be extended to incorporate multiple lactam bridges that are compatible with the PP fold.

CD spectra of the synthetic peptides in aqueous buffer at pH 5.0 (Figures 2 and 3) demonstrate that they self-associate in the micromolar concentration range with increasing  $\alpha$ -helical character, a general characteristic of

(38) Jorgensen, Ch. J.; Fuhlendorff, J.; Schwartz, T. W. Structure-Function Studies on Neuropeptide Y and Pancreatic Polypeptide—Evidence for Two PP-Fold Receptors in Vas Deferens. *Eur. J. Biochem.* 1990, 186, 105-114.

amphiphilic peptides.<sup>33</sup> Curve-fitting analyses of the experimental data according to eq 1 suggest that both NPY and *N*<sup>α</sup>-Ac-NPY(10–36) form dimers in this concentration range (Table I), although the data for NPY are also consistent with cooperative trimerization. Provencher analyses<sup>36</sup> of the CD spectra at low concentrations indicate that the monomeric form of NPY retains 32%  $\alpha$ -helical structure in aqueous solution at 25 °C, and a similar value (30%) is estimated from the mean residue ellipticity at 222 nm (Table II). These results are consistent with those reported previously for monomeric NPY in 160 mM KCl solution at pH 7.5.<sup>14</sup> In contrast, the monomeric form of *N*<sup>α</sup>-Ac-NPY(10–36) is estimated to have only 13% or 19%  $\alpha$ -helix using these methods. If structures other than the  $\alpha$ -helical domain are correctly accounted for by the Provencher analysis and do not contribute significantly to the ellipticity at 222 nm, and if the  $\alpha$ -helix is located within residues 13 to 36 (see below), then the monomeric form of *N*<sup>α</sup>-Ac-NPY(10–36) would be expected to have a higher  $\alpha$ -helix content than that of NPY on a per residue basis. Together, therefore, these results are consistent with a significant fraction (about half) of the NPY molecules adopting a weakly stable, globular conformation in solution comparable to that described by the PP fold.<sup>12</sup>

Results from the CD experiments also clearly demonstrate the helix-stabilizing effect of the [Lys<sup>n</sup>,Asp<sup>n+4</sup>] lactam bridge when introduced into the amphiphilic  $\alpha$ -helical segment of *N*<sup>α</sup>-Ac-NPY(10–36). Such helix stabilizing effects have also been observed when similar constraints were introduced into amphiphilic  $\alpha$ -helical domains of GRF analogues<sup>26,27</sup> and model peptides.<sup>28</sup> It appears, therefore, that this particular conformational constraint has an intrinsic ability to stabilize the  $\alpha$ -helical conformation that is a priori largely independent of the local amino acid sequence.

Meaningful comparisons between the N-terminal deleted analogues and the full-length peptides can be made if the  $\alpha$ -helix contents for the monomeric forms of the peptides (Table I) are recalculated on a per residue basis that includes only residues 13–36. Such a recalculation makes the reasonable assumption that none of the peptides have  $\alpha$ -helical structure in the proline-rich region comprising residues 1–12. Using the data from the Provencher analyses, NPY and *N*<sup>α</sup>-Ac-*cyclo*<sup>18,22</sup>-[Lys<sup>18</sup>,Asp<sup>22</sup>]-NPY(10–36) are calculated to be 48% and 57%  $\alpha$ -helical, respectively, in residues 13–36. These values suggest that the helix-stabilizing effect of the lactam bridge is comparable to that of the polyproline II-like helix in the PP fold. Furthermore, if the helix content of monomeric *N*<sup>α</sup>-Ac-NPY(10–36) is recalculated in the same way, giving 15% for residues 13–36, the change in free energy for the coil to helix transition that results from substituting the lactam bridge into this peptide may be estimated as -1.2 kcal/mol.

In contrast to the results obtained for the N-terminal deleted analogues, monomeric *cyclo*<sup>18,22</sup>-[Lys<sup>18</sup>,Asp<sup>22</sup>]-NPY was somewhat less helical than monomeric NPY (Figure 3B and Table II). This suggests that the [Lys<sup>18</sup>,Asp<sup>22</sup>] bridge, which is located at the boundary between the hydrophobic and hydrophilic faces of the amphiphilic  $\alpha$ -helix, may interfere with packing of the polyproline II-like helix against the  $\alpha$ -helix and disrupt the PP fold. A somewhat analogous "negative cooperativity" between two  $\alpha$ -helix stabilizing structural elements (both lactam bridges) incorporated into widely separated segments of GRF analogues has been reported previously.<sup>27</sup> Both cases illustrate the considerations for long-range interactions, presumably involving folded conformations, that must be taken into account in designing such lactam-bridged peptide ana-

logues for optimal helix stabilization.

Results from competitive binding assays in rat cortical membranes (Table III) indicate that the presence of the [Lys<sup>18</sup>,Asp<sup>22</sup>] bridge in the proposed  $\alpha$ -helical region is compatible with receptor recognition. The reduced receptor affinities of the N-terminal truncated analogues relative to the full-length analogues and the slightly reduced affinity of *cyclo*<sup>18,22</sup>-[Lys<sup>18</sup>,Asp<sup>22</sup>]-NPY in comparison to NPY, can both be rationalized in terms of the functional importance of the proposed PP fold. Figure 1A illustrates how the PP fold causes the N- and C-terminal ends to be in close spatial proximity and generates a striking distribution of charged residues. In fact, all six of the positively charged residues and all five of the negatively charged residues are completely segregated in opposite ends of the folded molecule in this conformation. Current structure-activity relationship studies on NPY<sup>19,21,39,40</sup> have demonstrated the importance of both the N- and C-terminal residues for receptor recognition and activation, suggesting that the PP fold provides the tertiary structural organization required for NPY to approach its receptor in the correct conformation for recognition, directed by long-range electrostatic interactions. Since monomeric *N*<sup>α</sup>-Ac-NPY(10–36) has clearly lost most of the conformation characterizing the PP fold in aqueous solution (Figure 3) in addition to the loss of receptor interactions due to deletions of the N-terminal residues, the lower affinity of this peptide in comparison to NPY is not surprising. In this regard, even deletion of Tyr<sup>1</sup> has been shown to reduce the potency of NPY significantly in various bioassays.<sup>18,19,21</sup> The lower affinity of *cyclo*<sup>18,22</sup>-[Lys<sup>18</sup>,Asp<sup>22</sup>]-NPY compared to NPY may result from the apparent disruptive effect of the lactam bridge on the PP fold that is indicated by the CD results, as described above. This would reduce the efficiency of receptor location by the proposed electrostatic mechanism, and may also disrupt the spatial relationship between the N- and C-terminal residues that is required for high-affinity binding.

The receptor-binding potencies of *N*<sup>α</sup>-Ac-NPY(10–36) and its helix-stabilized cyclic analogue are identical (Table III), indicating that the  $\alpha$ -helical conformation is probably the correct functional conformation for the lactam-bridged region. However, the  $\alpha$ -helix stabilization calculated for this proposed functional conformation of NPY residues 13–32 is about -1.2 kcal/mol, which would be expected to enhance the potency of *N*<sup>α</sup>-Ac-NPY(10–36) by about 7-fold. This suggests that the lactam bridge itself may be interfering with receptor binding to a small extent, either directly or by distorting the helix from its preferred bound conformation.

In the rat vas deferens assays (Table III), the N-terminal truncated analogues are also less potent than the full-length analogues. However, by comparison with the brain receptor binding assays, both of the lactam-bridged analogues are more potent than expected relative to the corresponding linear peptides. Thus, *cyclo*<sup>18,22</sup>-[Lys<sup>18</sup>,Asp<sup>22</sup>]-NPY is equipotent with NPY in the vas deferens, although its affinity for NPY receptors in the brain is lower. Similarly, *N*<sup>α</sup>-Ac-*cyclo*<sup>18,22</sup>-[Lys<sup>18</sup>,Asp<sup>22</sup>]-

(39) Cox, H. M.; Krstenansky, J. L. The Effects of Selective Amino Acid Substitution Upon Neuropeptide Y Antisecretory Potency in Rat Jejunum Mucosa. *Peptides* 1991, 12, 323–327.

(40) Schwartz, T. W.; Fuhlendorff, J.; Langeland, N.; Thøgersen, H.; Jørgensen, Ch. J.; Sheikh, S. P. Y<sub>1</sub> and Y<sub>2</sub> Receptors for NPY—The Evolution of PP-Fold Peptides and Their Receptors. In *Neuropeptide Y*; Mutt, V., Fuxe, K., Hokfelt, T., Lundberg, J. M., Eds.; Raven Press: New York, 1989; pp 143–151.



NPY(10-36) is over 2-fold more potent than  $N^{\alpha}$ -Ac-NPY-(10-36) in this assay, although these two peptides are equipotent in the brain receptor binding assay. The presynaptic NPY receptors responsible for activity in the rat vas deferens assays have been classified as  $Y_2$ ,<sup>38</sup> and rat brain cortex has been assumed to contain in large part the  $Y_2$  receptor.<sup>40</sup> If the NPY receptors involved in each system are indeed the same, this suggests that the conformationally restricted analogues may be characterized by an increased efficacy (efficiency of receptor activation upon binding) in comparison to the linear peptides. In this case, it remains to be determined whether the  $\alpha$ -helical conformation per se, or its propagated effect on the C-terminal residues, is more important.

In summary, we have demonstrated the presence of a folded conformation in a significant fraction of monomeric NPY molecules in aqueous solution at 25 °C, in which the proline-rich sequence 1-9 stabilizes  $\alpha$ -helical structure in the C-terminal half of the molecule. This conformation is likely to be similar to the PP fold that has been proposed as the functional conformation of NPY. The helix-stabilizing effect noted elsewhere<sup>26-28</sup> of a lactam bridge linking the side chains of Lys<sup>n</sup> to Asp<sup>n+4</sup> has also been confirmed. Such a bridge in positions 18 and 22 of the amphiphilic  $\alpha$ -helical segment of NPY (residues 13-32) has been found to substitute effectively for residues 1-9 in stabilizing the helical structure. Results from pharmacological assays of the linear and cyclized NPY analogues are generally consistent with a receptor-binding role for the proposed PP fold, and indicate that stabilization of the amphiphilic helix may promote receptor activation.

## Experimental Section

**Synthesis. Reagents, Methods, and Instruments.** Protected amino acids (L configuration) were purchased from Bachem Inc. or Peninsula Laboratories. Solid-phase syntheses were carried out on *p*-methylbenzhydrylamine resin (0.60 mequiv of amino groups/g) (Peninsula Laboratories) and *p*-nitrobenzophenone oxime resin (0.12 mequiv of oxime groups/g) synthesized according to the literature.<sup>24,25,41</sup> DMF (Baxter) was distilled from ninhydrin under reduced pressure and stored over 4-Å molecular sieves. DIEA (Aldrich) was also distilled from ninhydrin. DCM and *i*-PrOH (ACS grade) were stored over 4-Å molecular sieves. TFA (Halocarbon), EtOH (Quantum Chemical Corp.), and  $\text{CHCl}_3$ , EtOAc, and MeOH (Fisher Scientific) were used without further purification. Ethyl 2-(hydroxyimino)-2-cyanoacetate (EACNO<sub>2</sub>) was synthesized according to the literature.<sup>42</sup> HOBt·H<sub>2</sub>O, TFE, DIC, and Zn dust were purchased from Aldrich, DCC from Fluka, Sephadex G-15 (40-120  $\mu\text{m}$ ) from Pharmacia, and silica gel for flash chromatography from Baker.

Peptides were hydrolyzed in 6 N HCl (Pierce) at 110 °C for 24 h and peptidyl resins in 12 N HCl/propionic acid 1/1 (Pierce) at 130 °C for 24 h. Phenol was added for peptides containing tyrosine residues. Tests for racemization were done by reacting hydrolysates with 1-fluoro-2,4-dinitrophenyl-5-L-alanine amide (Pierce) followed by separation and quantification of the resulting diastereomers by reverse-phase HPLC on a Vydac C<sub>18</sub> analytical column according to the literature.<sup>43</sup> Values are given as percentage of D-amino acid content and are not corrected for racemization due to acid hydrolysis.<sup>44</sup> Mass spectra were determined using the <sup>252</sup>Cf fission fragment and electrospray techniques. TLC

analyses were performed on precoated silica gel F-254, 0.25-mm plates (Aldrich) in the following solvent systems: (A) EtOAc/hexane 1/2, (B) *n*-BuOH/AcOH/water 4/1/1, (C) EtOAc/hexane 1/1, (D)  $\text{CHCl}_3$ /AcOH 9.5/0.5, (E) EtOAc/hexane 1/5, (F) EtOAc/hexane/AcOH 9.5/10/0.5, (G) acetone/hexane/AcOH 9.5/10/0.5, (H)  $\text{CHCl}_3$ /EtOH/dioxane/AcOH 14/0.8/7/0.6, (I)  $\text{CHCl}_3$ /MeOH/AcOH 85/10/5, and (J)  $\text{CHCl}_3$ /MeOH/AcOH 60/10/5. Spots were visualized with a UV lamp (254 nm) and/or by exposing to TFA vapor (for Boc-protected amino acids), spraying with a 2% solution of ninhydrin in acetone, and heating.

Optical rotations were measured with a Perkin-Elmer 241 polarimeter at room temperature. Melting points were taken on a Thomas Hoover apparatus and are not corrected. Amino acid analyses were performed with a Dionex 300 analyzer. Reverse-phase HPLC was done with a Waters 600 or Beckman 344 apparatus on Vydac C<sub>4</sub> and C<sub>18</sub> semipreparative (1.0 × 25 cm, 5  $\mu\text{m}$ ) and preparative (2.2 × 25 cm, 15-20  $\mu\text{m}$ ) columns, using flow rates of 3.0 and 10 mL/min, respectively. Eluents were as follows: A, 0.1% TFA in water; B, 0.1% TFA in 90%  $\text{CH}_3\text{CN}$ /water. Wavelength used for the detection of peaks was 220 nm.

**Asp-OPac Trifluoroacetate (1).** To a stirred solution of Boc-Asp(O<sup>t</sup>Bu)-OH (3.79 g, 13.1 mmol) in EtOAc (26 mL) were added TEA (1.83 mL, 13.1 mmol) and 2-bromoacetophenone (Pac-Br; 2.61 g, 13.1 mmol). The mixture was stirred overnight at room temperature and worked up according to the literature method.<sup>45</sup> crude yield 5.26 g (99%); an analytical sample crystallized from EtOAc/hexane had mp 62-63 °C;  $[\alpha]_D -11.8^\circ$  (c 0.88, MeOH); TLC  $R_f$ (A) 0.60. This product (2.60 g, 6.39 mmol) was dissolved in TFA (15 mL) and stirred for 1 h at room temperature. Compound 1 was precipitated by the slow addition of ether (14 mL), filtered, washed with ether, and dried: yield 2.16 g (93%); mp 113-114 °C;  $[\alpha]_D -6.28^\circ$  (c 1.3, MeOH); TLC  $R_f$ (B) 0.74. Anal. Calcd for C<sub>14</sub>H<sub>14</sub>N<sub>1</sub>O<sub>7</sub>Fe<sub>3</sub>(365.3): C, 46.03; H, 3.87; N, 3.84. Found: C, 46.01; H, 3.87; N, 3.51.

**Boc-Tyr(Br-Z)-Asp-OPac (3).** Boc-Tyr(Br-Z)-OSu (2) was prepared from Boc-Tyr(Br-Z)-OH according to the literature method.<sup>46</sup> Compound 1 (2.49 g, 6.8 mmol) was then dissolved in water (66 mL), cooled to 0 °C, and NaHCO<sub>3</sub> (1.15 g, 13.7 mmol) was added. To this solution was added an ice-cold solution of compound 2 (3.73 g, 6.3 mmol) in 1,2-dimethoxyethane (53 mL) followed by more NaHCO<sub>3</sub> (0.53 g, 6.3 mmol) and ice-cold 1,2-dimethoxyethane (60 mL). After stirring for 2 days at 4 °C, the solution was acidified at 0 °C with ice-cold 0.5 N HCl to pH 3. Crude compound 3 precipitated out and the suspension was extracted with EtOAc (4 × 35 mL). The combined organic extracts were washed, at 0 °C, with 0.05 N HCl (3 × 30 mL) and water (3 × 40 mL), dried over anhydrous Na<sub>2</sub>SO<sub>4</sub>, and evaporated to a yellow foam. Crude peptide 3 was purified by flash chromatography in EtOAc/hexane/AcOH 9.9/10/0.1. The fractions corresponding to the desired product were pooled, evaporated, and recrystallized from EtOAc/ether: yield 3.24 g (71%); mp 103-105 °C;  $[\alpha]_D +26.6^\circ$  (c 1.2,  $\text{CHCl}_3$ ); TLC  $R_f$ (D) 0.31. Anal. Calcd for C<sub>34</sub>H<sub>35</sub>N<sub>2</sub>O<sub>11</sub>Br<sub>1</sub> (727.56): C, 56.12; H, 4.86; N, 3.85. Found: C, 56.53; H, 4.87; N, 3.83.

**Boc-Lys(Trt)-OH (4).** To a stirred solution of Boc-Lys-OMe acetate (Bachem) (0.50 g, 1.5 mmol) in dry  $\text{CHCl}_3$  (10 mL) at 0 °C were added TEA (0.45 mL, 3.2 mmol) and triphenylmethyl chloride (Trt-Cl; 0.422 g, 1.5 mmol). After 15 min, the mixture was warmed up to room temperature and stirred for an additional 6 h. The solution was then washed at 0 °C with water (3 × 10 mL), 5% citric acid (3 × 10 mL), and water (3 × 10 mL), dried over anhydrous Na<sub>2</sub>SO<sub>4</sub>, and evaporated to a yellow oil: crude yield 0.48 g (65%); a chromatographically pure sample had  $[\alpha]_D +26.3^\circ$  (c 1.3,  $\text{CHCl}_3$ ); TLC  $R_f$ (E) 0.38  $R_f$ (F) 0.92. This product (3.17 g, 6.3 mmol) was dissolved in MeOH (3.2 mL) and cooled to 0 °C, and 2.0 N NaOH in MeOH (3.2 mL, 6.3 mmol) was added. After 11 h at 4 °C, water (103 mL) was added and the mixture acidified, at 0 °C, with ice-cold 30% aqueous AcOH to pH 4. The

- (41) Findeis, M. A.; Kaiser, E. T. Nitrobenzophenone Oxime Based Resins for the Solid-Phase Synthesis of Protected Peptide Segments. *J. Org. Chem.* 1989, 54, 3478-3482.  
 (42) Conrad, M.; Schultz, A. Über Nitroso-cyanessigsäure-derivate. *Ber. Dtsch. Chem. Ges.* 1909, 42, 735-737.  
 (43) Marfey, P. Determination of D-Amino Acids. II. Use of a Bifunctional Reagent, 1,5-Difluoro-2,4-dinitrobenzene. *Carlsberg Res. Commun.* 1984, 49, 591-596.  
 (44) Frank, H.; Woiwode, W.; Nicholson, G.; Bayer, E. Determination of the Rate of Acid Catalyzed Racemization of Protein Amino Acids. *Liebigs Ann. Chem.* 1981, 354-365.

- (45) Stelakatos, G. C.; Paganou, A.; Zervas, L. New Methods in Peptide Synthesis. Part III. Protection of Carboxyl Group. *J. Chem. Soc. C* 1966, 1191-1199.  
 (46) Daoust, H.; St-Pierre, S. Synthesis and Conformation of Sequential Polypeptides Containing  $\epsilon$ -Benzoyloxycarbonyl-Lysine and Benzyl Esters of Aspartic and Glutamic Acids. *J. Chem. Soc., Perkin Trans. 1* 1976, 1453-1457.

resulting precipitate was filtered, washed with ice-cold water several times, and dried. Crude 4 was purified by flash chromatography in EtOAc/hexane/AcOH 9.75/10/0.25. The fractions corresponding to the desired product were pooled, evaporated, and dried: yield 1.76 g (57%);  $[\alpha]_D +6.52^\circ$  (c 0.79, CHCl<sub>3</sub>); TLC  $R_f$ (F) 0.35 and  $R_f$ (G) 0.71; racemization test 5% D-Lys. Anal. Calcd for C<sub>30</sub>H<sub>36</sub>N<sub>2</sub>O<sub>4</sub> (488.63): C, 73.73; H, 7.44; N, 5.73. Found: C, 69.84; H, 7.48; N, 5.03.

**Boc-Lys(Trt)-Arg(Tos)-Tyr(Br-Z)-Tyr(Br-Z)-Asp(O-resin)-OPac (6).** A DCC solution (0.49 M in DCM, 5.8 mL, 2.86 mmol) was added to a mixture of protected peptide 3 (2.04 g, 2.81 mmol), EACNO<sub>2</sub> (0.81 g, 5.71 mmol), and Kaiser oxime resin (17 g, 0.12 mequiv/g) in DCM (60 mL). After mixing for 30 min at -10 °C and for 24 h at room temperature, peptidyl resin 5 was washed with DCM (4×), DCM/EtOH 2/1 (3×), and EtOH (4×) and dried over P<sub>2</sub>O<sub>5</sub> under vacuum: yield 1.75 mmol of peptide (86%); substitution level 0.094 mequiv/g of resin, based on picric acid determination.<sup>47</sup> Peptidyl resin 5 was then acylated with Ac<sub>2</sub>O (0.58 mL, 6.12 mmol) and DIEA (1.07 mL, 6.12 mmol) in DCM (119 mL) for 1 h. Subsequent couplings were carried out according to the standard protocol for stepwise peptide synthesis on Kaiser oxime resin.<sup>24</sup> The following coupling methods were used: Boc-Tyr(Br-Z)-OH as preformed symmetrical anhydride (5 equiv) and DIEA (2.2 equiv) (in situ neutralization) in DCM (50 mL); Boc-Arg(Tos)-OH (4 equiv), DCC (4 equiv), and HOBT·H<sub>2</sub>O (7 equiv) in DCM/DMF 1/1 (58 mL); 4 (1.3 equiv), DCC (1.3 equiv), and HOBT·H<sub>2</sub>O (2.6 equiv) in DCM/DMF 1/1 (57 mL). Coupling and deprotection steps were monitored by the Kaiser ninhydrin test.<sup>48</sup>

**Cyclization Reaction: *cyclo*<sup>1,5</sup>Boc-Lys-Arg(Tos)-Tyr(Br-Z)-Tyr(Br-Z)-Asp-OPac (7).** Selective removal of N<sup>ε</sup>-Trt protecting group from peptidyl resin 6 (1.07 mmol of Trt group, based on picric acid determination<sup>47</sup>) was achieved in 5% TFA in DCM/TFE 1/1 (220 mL). This reaction was monitored by following the absorbance of the released Trt carbocation at 404 nm. After 3 h, a constant absorbance value was reached and the reaction was judged complete. A yield of 85% was calculated using  $\epsilon_{404} = 33\,500\text{ M}^{-1}\text{ cm}^{-1}$  for the Trt carbocation. The peptidyl resin was then drained, washed with TFE/DCM 1/1 (2×), DCM (2×), *i*-PrOH (2×), and DCM (3×), and neutralized with 5% DIEA/DCM (4×) followed by more washes with DCM (4×). Side-chain to side-chain cyclization was carried out in DCM (119 mL) in the presence of AcOH (79  $\mu$ L, 1.4 mmol) for 65 h at room temperature. Protected cyclic peptide was obtained by draining the reaction vessel and washing the resin with DCM (3×), DCM/EtOH 2/1 (3×), EtOH (2×), and DCM (2×). The combined filtrate was evaporated and two UV-active spots were detected by TLC:  $R_f$ (H) 0.44 and  $R_f$ (I) 0.88. Crude peptide 7 was purified by flash chromatography in solvent system (H) followed by reverse-phase HPLC on a Vydac C<sub>4</sub> preparative column using a linear gradient of 57% B to 92% B in 30 min. Fractions corresponding to desired peptide, eluting at 77% B, were collected, evaporated, and lyophilized: yield 467 mg, 29%;  $[\alpha]_D -0.52^\circ$  (c 1.2, DMF); TLC  $R_f$ (H) 0.44; amino acid analysis Arg (1) 1.06, Asp (1) 1.00, Lys (1) 0.90, Tyr (2) 2.23; MS <sup>252</sup>Cf fission fragment (M + Na)<sup>+</sup> = 1547.3 (calcd = 1547.2,  $\Delta = +0.1$ ).

The covalent cyclic dimer of 7 was identified as the other main product of the cyclization reaction: yield 233 mg, 14%; molar ratio of monomer/dimer = 4/1;  $[\alpha]_D -5.14^\circ$  (c 1.1, DMF); TLC  $R_f$ (H) 0.88; amino acid analysis Arg (2) 1.84, Asp (2) 2.00, Lys (2) 1.90, Tyr (4) 4.80; MS <sup>252</sup>Cf fission fragment (2M + Na)<sup>+</sup> = 3071.4 (calcd = 3071.4,  $\Delta = 0.0$ ).

Overall yield for cyclization reaction, including monomer and dimer formation, was 43%.

***cyclo*<sup>1,5</sup>Boc-Lys-Arg(Tos)-Tyr(Br-Z)-Tyr(Br-Z)-Asp-OH (8).** Protected cyclic peptide 7 (384 mg, 252  $\mu$ mol) was dissolved in 90% AcOH (6 mL), and Zn dust (0.50 g, 7.6 mmol) was added to the vigorously stirred solution at room temperature. The

reaction was followed by TLC in solvent system (I) and was judged completed after 1 h. Zn was removed by filtration and washed with 90% AcOH, and the filtrate was evaporated to an oil. Crude peptide 8 was purified by reverse-phase HPLC on a Vydac C<sub>4</sub> preparative column using a linear gradient of 30% B to 80% B in 45 min. Fractions corresponding to the desired compound, eluting at 75% B, were pooled, evaporated, and lyophilized: yield 320 mg, 90%;  $[\alpha]_D +6.5^\circ$  (c 1.7, DMF); TLC  $R_f$ (J) 0.48; amino acid analysis Arg (1) 0.84, Asp (1) 1.00, Lys (1) 0.92, Tyr (2) 1.94; MS <sup>252</sup>Cf fission fragment (M + Na)<sup>+</sup> = 1406.3 (calcd = 1406.1,  $\Delta = +0.2$ ); racemization test 6% D-Lys and 3% D-Asp. Anal. Calcd for C<sub>64</sub>H<sub>72</sub>N<sub>6</sub>O<sub>19</sub>Br<sub>2</sub>S<sub>1</sub>F<sub>3</sub> (1520.18): C, 50.57; H, 4.77; N, 8.29. Found: C, 50.16; H, 4.89; N, 8.33.

**Segment Condensation: Boc-(protected cyclic segment)-(NPY(23-36))-*p*-MBHA Resin (9).** NH<sub>2</sub>-(NPY(23-36))-*p*-MBHA resin was synthesized according to standard procedures for stepwise solid-phase peptide synthesis. Briefly, the neutralized *p*-MBHA resin (0.60 g, 0.60 mmol/g) was reacted with the preformed symmetrical anhydride to the C-terminal Boc-Tyr(Br-Z)-OH (0.134 g, 0.27 mmol) in DCM (3 mL) overnight: substitution level 0.184 mequiv/g resin, based on picric acid determination.<sup>47</sup> The resin was then acetylated with Ac<sub>2</sub>O (0.34 mL, 3.60 mmol) and DIEA (0.63 mL, 3.60 mmol) in DCM (4 mL) for 1 h. The following amino acid derivatives were used for subsequent couplings: Boc-Ala, Boc-Arg(Tos), Boc-Asn, Boc-Gln, Boc-Ile-<sup>1</sup>/<sub>2</sub>H<sub>2</sub>O, Boc-His( $\pi$ -Bom), Boc-Leu-H<sub>2</sub>O, Boc-Thr(Bzl), and Boc-Tyr(Br-Z). Couplings were done using the preformed symmetrical anhydride method, except for Boc-Asn, Boc-Gln, Boc-Arg(Tos), and Boc-His( $\pi$ -Bom), which were reacted as the preformed hydroxybenzotriazole active esters: substitution level 0.121 mequiv/g of resin, based on Ala; amino acid analysis Ala (1) 1.00, Arg (3) 2.58, Asn (1) 1.00, Gln (1) 1.15, His (1) 0.84, Ile (2) 1.80, Leu (2) 1.96, Thr (1) 0.56, Tyr (2) 1.73.

A DCC solution (0.49 M in DCM, 242  $\mu$ L, 119  $\mu$ mol) was added to a mixture of protected cyclic peptide 8 (153 mg, 111  $\mu$ mol), EACNO<sub>2</sub> (34 mg, 240  $\mu$ mol), and NH<sub>2</sub>-(NPY(23-36))-*p*-MBHA resin (0.66 g, 80  $\mu$ mol) in DCM (3 mL). The mixture was shaken for 30 min at -10 °C and for 24 h at room temperature after which it was reactivated with DCC (242  $\mu$ L, 119  $\mu$ mol) and DIEA (14  $\mu$ L, 80  $\mu$ mol). After 72 h, the peptidyl resin was washed with DCM (3×), DCM/EtOH 2/1 (2×), and DCM (3×). A positive Kaiser ninhydrin test was obtained and the peptidyl resin was then reacylated with peptide 8 (53 mg, 39  $\mu$ mol), EACNO<sub>2</sub> (1 mg, 78  $\mu$ mol), and DCC (81  $\mu$ L, 40  $\mu$ mol) according to the above procedures. After 72 h, peptidyl resin 9 was washed, acetylated with Ac<sub>2</sub>O (0.15 mL, 1.59 mmol) and DIEA (0.28 mL, 1.6 mmol) in DCM (6 mL) for 2 h, washed, and dried: coupling yield 60%, based on Lys/Ala ratio; substitution level 0.057 mequiv/g of resin, based on Lys; amino acid analysis Ala (1) 1.00, Arg (4) 3.46, Asn (2) 1.74, Gln (1) 1.27, His (1) 0.68, Ile (2) 1.98, Leu (2) 2.21, Lys (1) 0.60, Thr (1) 0.93, Tyr (4) 3.27.

**Cyclic Peptides: N<sup>ε</sup>-Ac-*cyclo*<sup>18,22</sup>[Lys<sup>18</sup>,Asp<sup>22</sup>]-NPY(10-36) (10) and *cyclo*<sup>18,22</sup>[Lys<sup>18</sup>,Asp<sup>22</sup>]-NPY (11).** Cyclic peptides 10 and 11 were assembled by performing repetitive coupling cycles on peptidyl resin 9 using the following amino acid derivatives: Boc-Ala, Boc-Asn, Boc-Asp(Bzl), Boc-Gly, Boc-Lys(2-Cl-Z), Boc-Pro, Boc-Ser(Bzl), and Boc-Tyr(Br-Z). Coupling procedures were as described above. A portion of the resin was removed at the appropriate time during this synthesis and acetylated using excess Ac<sub>2</sub>O and DIEA in DCM for 10. Peptides were then cleaved from the support by treatment with HF/anisole for 30 min at -10 °C and for 30 min at 0 °C. The resulting crude peptide 10 and 11 mixtures were washed with ethyl ether (3 × 10 mL), extracted with 20% AcOH (3 × 10 mL), and lyophilized. The crude peptides, dissolved in 0.2 N AcOH, were applied to a column of Sephadex G-15 (2.5 × 50 cm) and eluted with 0.2 N AcOH. Peptides were detected by absorbance measurements at 274 nm. Fractions comprising the major peak were pooled, evaporated, and lyophilized. Crude peptides were further purified by reverse-phase HPLC on a Vydac C<sub>18</sub> semipreparative column using a linear gradient of 27% B to 31% B in 27 min followed by 31% B to 44% B in 27 min for 10 and 27% B to 40% B in 50 min for 11. Fractions corresponding to the desired peptides, eluting at 42% B for 10 and 39% B for 11, were collected, evaporated, and lyophilized: amino acid analysis 10 Ala (3) 3.00, Arg (4) 4.21, Asx (4) 4.10, Glx (3) 3.35, His (1) 1.00, Ile (2) 2.05, Leu (3) 3.05, Lys

(47) Gisin, B. F. The monitoring of Reactions in Solid-Phase Peptide Synthesis with Picric Acid. *Anal. Chim. Acta* 1972, 58, 248-249.

(48) Kaiser, E.; Colescott, R. L.; Bossinger, C. D.; Cook, P. I. Color Test for Detection of Free Terminal Amino Groups in the Solid-Phase Synthesis of Peptides. *Anal. Biochem.* 1970, 34, 595-598.

(1) 0.92, Pro (1) 1.16, Thr (1) 1.19, Tyr (4) 4.56, and 11 Ala (3) 3.00, Arg (4) 3.72, Asx (6) 6.24, Glx (3) 3.04, Gly (1) 1.40, His (1) 0.93, Ile (2) 1.76, Leu (3) 2.86, Lys (2) 1.91, Pro (4) 3.63, Ser (1) 1.13, Thr (1) 0.83, Tyr (5) 4.03; MS electrospray 10 (M + 4H)<sup>4+</sup> = 3406.6 (calcd = 3406.8,  $\Delta$  = -0.2), and 11 (M + 6H)<sup>8+</sup> = 4320.3 (calcd = 4320.8,  $\Delta$  = -0.5). Purity of peptides was checked by reverse-phase HPLC on a Vydac C<sub>18</sub> analytical column. (No evidence for additional glycine residues in 11 was obtained from the mass spectrum. The high value for Gly obtained by amino analysis of 11 is probably an artefact resulting from the small peak size and buffer impurities.)

**Linear Peptides: N<sup>α</sup>-Ac-NPY(10-36) (12) and NPY (13).** Linear peptides 12 and 13 were synthesized and purified using the same methodology as for peptides 10 and 11: amino acid analysis 12 Ala (4) 4.00, Arg (4) 3.77, Asx (3) 3.06, Glx (3) 2.89, His (1) 1.00, Ile (2) 1.56, Leu (3) 2.98, Pro (1) 1.10, Ser (1) 1.16, Thr (1) 0.93, Tyr (4) 2.09, and 13 Ala (4) 4.00, Arg (4) 4.54, Asx (5) 5.02, Glx (3) 2.68, Gly (1) 1.13, His (1) 1.07, Ile (2) 1.91, Leu (3) 3.02, Lys (1) 1.07, Pro (4) 3.5, Ser (2) 1.70, Thr (1) 1.03, Tyr (5) 4.64; MS <sup>252</sup>Cf fission fragment 12 (M + H)<sup>+</sup> = 3340.7 (calcd = 3340.6,  $\Delta$  = +0.1), and 13 (M + H)<sup>+</sup> = 4254.1 (calcd = 4254.6,  $\Delta$  = -0.5). Purity of peptides was checked by reverse-phase HPLC on a Vydac C<sub>18</sub> analytical column.

**Circular Dichroism Spectroscopy.** Circular dichroism (CD) spectra were recorded on an Aviv 62 ds spectropolarimeter. For the concentration dependency studies, spectral data represent the average of 15 scans obtained between 210 and 207 nm with a bandwidth of 1.5 nm and a time constant of 5 s (scan rate 6 nm/min). Other spectra represent the average of 10 scans recorded in the range between 240 and 190 nm with a bandwidth of 1.5 nm and a time constant of 2 s (scan rate 3 nm/min). The cylindrical quartz cells (1.0-mm, 5.0-mm, and 20-mm pathlength) used in all CD measurements were acid washed, soaked in 1% aqueous polyethylene glycol solution (MW 15-20 kD), and then rinsed with water before use. Peptide solutions buffered with 10 mM sodium phosphate (pH 5.0) were used at 25-26 °C. Concentrations of stock peptide solutions in water were determined by absorbance measurements in 6.0 M guanidine hydrochloride buffered with 20 mM phosphate (pH 6.5), using  $\epsilon_{275.5} = 1500 \text{ M}^{-1} \text{ cm}^{-1}$  for the tyrosyl residues.<sup>49</sup> Ellipticities are expressed on a molar basis as mean residue ellipticities.

**Sedimentation Equilibrium Experiments.** Sedimentation equilibrium experiments were performed on a Beckman Airfuge Ultracentrifuge.<sup>50</sup> Peptide solutions in 10 mM phosphate buffer (pH 5.0), containing 5 mg/mL dextran T-40, at concentrations of 170, 170, 200, and 75  $\mu\text{M}$  were used for N<sup>α</sup>-Ac-NPY(10-36), N<sup>α</sup>-Ac-cyclo<sup>18,22</sup>-[Lys<sup>18</sup>, Asp<sup>22</sup>]-NPY(10-36), NPY, and cyclo<sup>18,22</sup>-[Lys<sup>18</sup>, Asp<sup>22</sup>]-NPY, respectively. Concentrations of stock solutions, in water, were determined as described above. Peptide solutions (100  $\mu\text{L}$ ) were centrifuged at 90 000 rpm for 24 h in quintuplicate. A standard consisting of 5 mg/mL hemoglobin in 150 mM NaCl, 20 mM phosphate buffer (pH 7.2) was included in each run. The peptide concentration gradient was analyzed by measuring the absorbance at 230 nm of each successive 10- $\mu\text{L}$  aliquot removed from the centrifuge tube, after a 10-fold dilution with buffer. Molecular weights were obtained from the slope of a plot of ln (absorbance<sub>230</sub>) versus (radial distance).<sup>50</sup>

**Pharmacological Assays. Membrane Preparation.** Male Sprague-Dawley rats (250-300 g) from Charles River Breeding Laboratories were decapitated and the brains rapidly removed and kept on ice. The cerebral cortex was dissected out, freed from white matter, and transferred to 10 mL of ice-cold 0.32 M sucrose

in 5 mM Hepes (pH 7.4) in a loose-fitting glass homogenizer. The tissue was homogenized for 20 strokes followed by centrifugation (1200g, 10 min) at 0 °C. The resulting supernatant was removed and centrifuged (40000g, 45 min) at 0 °C. The pellets were washed with 10 mL of ice-cold sucrose solution, homogenized for 10 strokes, and recentrifuged (40000g, 20 min) at 0 °C. The supernatant was discarded, and the crude mitochondrial pellets were suspended in 10 mL of ice-cold 20 mM Hepes buffer (pH 7.4) and rehomogenized for 6 strokes to obtain an even suspension. The membrane preparation was then divided in 0.5-mL portions, rapidly frozen, and stored at -70 °C. The protein concentration was determined using the Bio-Rad protein assay (Bio-Rad) and found to be  $2.9 \pm 0.51 \text{ mg/mL}$ .

**Receptor Binding Assays.** Competitive binding experiments were carried out using fresh preparations of <sup>125</sup>I-Bolton Hunter-NPY (Amersham Corp.) in a total volume of 500  $\mu\text{L}$  in plastic microcentrifuge tubes (1.5 mL). Tubes were filled with binding buffer (20 mM Hepes buffer, pH 7.4, containing 137 mM NaCl, 2.68 mM KCl, 1.8 mM CaCl<sub>2</sub>, 1.05 mM MgCl<sub>2</sub>, 1 mg/mL glucose, 0.1% w/v BSA, and 0.05% w/v bacitracin), unlabeled peptide in binding buffer in the concentration range from 10<sup>-6</sup> M to 10<sup>-13</sup> M, <sup>125</sup>I-labeled peptide in binding buffer (approximately 20 000 cpm/tube, 12 pM), and membrane preparation (0.2 mg of protein/mL). After incubation for 1 h at 25 °C, binding was terminated by centrifuging the tubes in a Beckman Microcentrifuge (14000 $\times$ g, 1 min). The supernatant was aspirated and the tip of the tube containing the pellets was cut off and counted for <sup>125</sup>I in a Beckman Gamma 5500 counter. Specific binding was calculated as the difference between the amount of <sup>125</sup>I-labeled peptide bound in the absence (total binding) and presence (nonspecific binding) of 1  $\mu\text{M}$  unlabeled NPY and represented approximately 60% of total binding. IC<sub>50</sub> values were determined by linear regression analysis from a graph of probit of the percentage specific binding (in the range from 20% to 80%) versus log peptide concentration. Three to seven independent experiments were performed in which each experimental point was determined in triplicate.

**Rat Vas Deferens Assays.** Vasa deferentia from male Sprague-Dawley rats (250-300 g) were dissected out and carefully freed from connective tissues. Vasa deferentia were mounted in 10-mL tissue baths containing Krebs buffer (133 mM NaCl, 4.7 mM KCl, 2.5 mM CaCl<sub>2</sub>, 1.4 mM NaHPO<sub>4</sub>, 1.0 mM MgCl<sub>2</sub>, 16.3 mM NaHCO<sub>3</sub>, and 7.8 mM glucose) saturated with a 95% O<sub>2</sub>/5% CO<sub>2</sub> gas mixture and maintained at 37 °C. Muscle contractions were initiated by applying square wave voltage pulses (60 V, 0.1 Hz, and 0.6 ms) generated through a pair of platinum electrodes connected to a Grass stimulator (Grass S88). The tissues were allowed to equilibrate under an initial tension of 1.0 g until a constant response was obtained (approximately 1 h). Buffer in the organ baths was exchanged a few times during the equilibrium period. Dose-response curves were determined by consecutive additions of peptide solutions in water, containing 1% BSA, to obtain concentrations in the bath ranging from 2 to 1000 nM. The data were analyzed in terms of percentage of the maximal inhibitory response for each peptide. IC<sub>50</sub> values were determined by linear regression analysis from a graph of probit of the percentage maximum inhibition (in the range from 20% to 80%) versus log peptide concentration. Three to seven independent experiments were performed.

**Acknowledgment.** NPY and N<sup>α</sup>-Ac-NPY(10-36) were synthesized and purified by Mr. Teddy T. Liu. Mass spectra were determined in the Rockefeller University Mass Spectrometry Laboratory directed by Dr. Brian Chait. We thank Dr. Barbara Brodsky and Dr. Norma Greenfield for advice concerning the CD spectra of collagen. This research was supported by USPHS Grants GM38811 and DA04197.

(49) Edelhoch, H. Spectroscopic Determination of Tryptophan and Tyrosine in Proteins. *Biochemistry* 1967, 6, 1948-1954.

(50) Pollet, R. J.; Haase, B. A.; Standaert, M. L. Macromolecular Characterization by Sedimentation Equilibrium in the Preparative Ultracentrifuge. *J. Biol. Chem.* 1979, 254, 30-33.